DISCRETE CRACK MODELLING OF DAMAGE PROPAGATION IN COMPOSITES SUBJECTED TO LOW VELOCITY IMPACT

T.E. Tay[1], J. Zhi[1]

[1] Department of Mechanical Engineering, National University of Singapore
9 Engineering Drive 1, 117575, Singapore
Email: mpetayte@nus.edu.sg and Jie.zhi@u.nus.edu
Webpage: http://www.me.nus.edu.sg

Keywords: Discrete crack methods, Floating node method, low velocity impact, matrix cracking, delamination

Abstract
Understanding damage mechanisms developed in laminates during low velocity impact is critical for damage tolerance analysis of composite structure. However, many models employ continuum damage mechanics (CDM) in material property degradation and cohesive elements because the damage patterns are complex. Such models do not explicitly model the interactions between numerous matrix cracks and delaminations because until now, the computational expense is too great. In this paper, the novel enhanced *Floading Node Method* is formulated in a geometrically nonlinear framework and used to numerically and explicitly model impact damage, including the initiation and propagation of discrete intra-layer and inter-layer cracks. The predicted internal damage patterns and structural response curve show good agreement with experimental results.

1. Introduction

Barely Visible Impact Damage (BVID) in laminated composites can develop during accidental impact events, such as dropped tool and runway debris. Therefore, damage characterization and impact resistance analysis become critical. Generally, either low-velocity impact (LVI) or quasi-static indentation test is utilized for the study of BVID, such as matrix cracking and delamination [1].

Besides experimental tests, numerical simulations are usually adopted for a better understanding of damage growth mechanism in composites [2-4]. Some recent work model the matrix-dominated failure implicitly with continuum damage mechanics (CDM) while the interfacial delamination is modelled as physical cracks with cohesive zone model (CZM) [5,6]. However, the approach requires pre-positioning parallel strips of cohesive elements within the ply material and the number of the strips has to be pre-defined manually before the analysis. To overcome such limitations, the *Floating Node Method* (FNM), first proposed by Chen et al. [7], which models multiple discrete discontinuities within finite elements, is extended in this paper to model impact-induced damage. An implicit dynamic procedure is developed with consideration of geometrical non-linearity. The proposed formulation is demonstrated by modelling the impact response of cross-ply laminates [4] as a case study. Coherent simulation results with experiments in terms of force-time curves and damage patterns are obtained.

2. Failure mechanisms for BVID

A comprehensive understanding of damage processes and governing mechanisms during impact event is necessary for the development of a reliable BVID predictive model, which is also relevant to the study of residual strength of composite structures. Complex damage patterns consisting of matrix

cracking, delamination and fiber breakage may occur during impact. Experiments have shown that a certain threshold value of impact energy exists, below which only small indentations could be observed at the impact point of laminates without any visible surface damage. Higher impact energy could result in fiber breakage at the surfaces. In both cases however, significant internal matrix cracking and delamination are usually formed, resulting in substantially reduced residual strength as determined by compression after impact (CAI) tests.

Standard tests have been developed to characterize LVI damage with a hemispherical impactor, as shown in Fig. 1 (a). Matrix cracking in the form of matrix micro-cracking and fiber/matrix debonding is usually observed as the first type of damage patterns. Generally, two kinds of matrix cracks initiate and propagate along fiber direction as shown in Fig. 1 (b). The vertical matrix cracks in the bottom layer due to tensile bending stresses are termed *bending cracks*, while inclined cracks within the laminate referred to as *shear cracks* are induced by transverse shear stresses. As these cracks reach the interface between plys, delaminations are induced. Fig. 1 (c) illustrates the delamination pattern induced by *bending cracks*, which appears in a peanut shape with the major axis along fiber direction of the layer right below the interface. The delamination propagation mainly driven by the interlaminar longitudinal shear stress (along fiber direction of the below layer) dissipates most energy absorbed in the laminate during LVI.

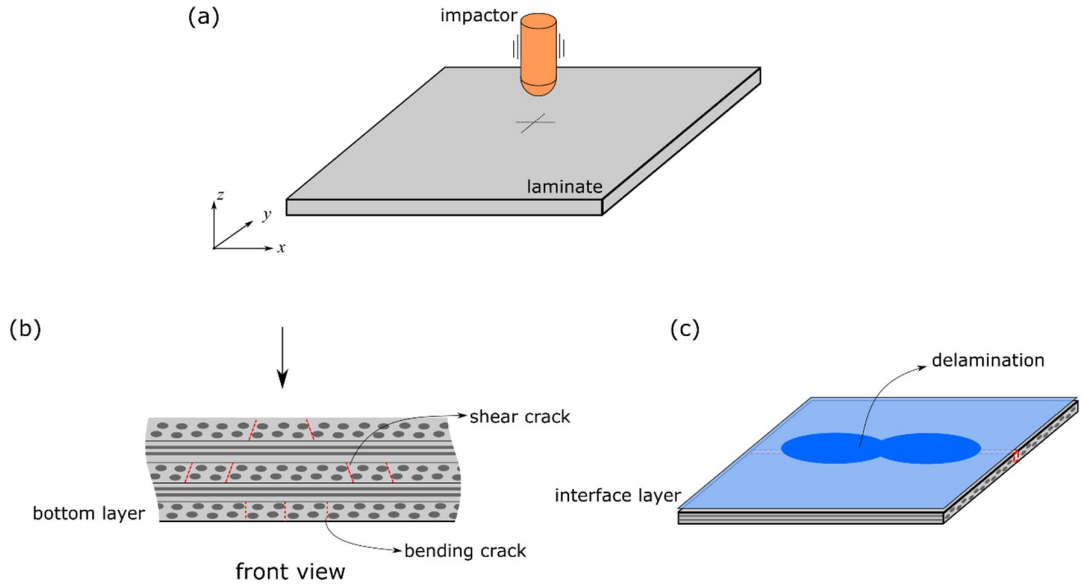

Figure 1. (a) A laminate subjected to low velocity impact; (b) Matrix cracking; (c) Delamination.

3. Discrete crack modeling of LVI on laminate plates

3.1. Floating node method

The *Floating Node Method* (FNM) belongs to a class of discrete crack models which aim at describing crack kinematics explicitly within finite elements. Extensions of the 3D FNM [7] to geometrically nonlinear framework with consideration of inertial effects are presented in this section. Two ingredients of the FNM are enriched solid element and enriched cohesive element, which are used for discretizing composite layers and interface layers, respectively, with the capability of capturing

matrix cracking, delamination and their interaction. Enrichements of discontinuities within continuum element are achieved with *floating nodes* pre-defined within node connectivity of an enriched element. As shown in Fig. 2 (a) and (b), extra nodes are allocated to eight edges (two nodes per edge) of brick elements and the location of these nodes are not pre-defined until certain damage or crack initiation criterion is satisfied based on the stress state. A possible scenario is illustrated in Fig. 2 (c) and (d) for solid and cohesive elements, respectively.

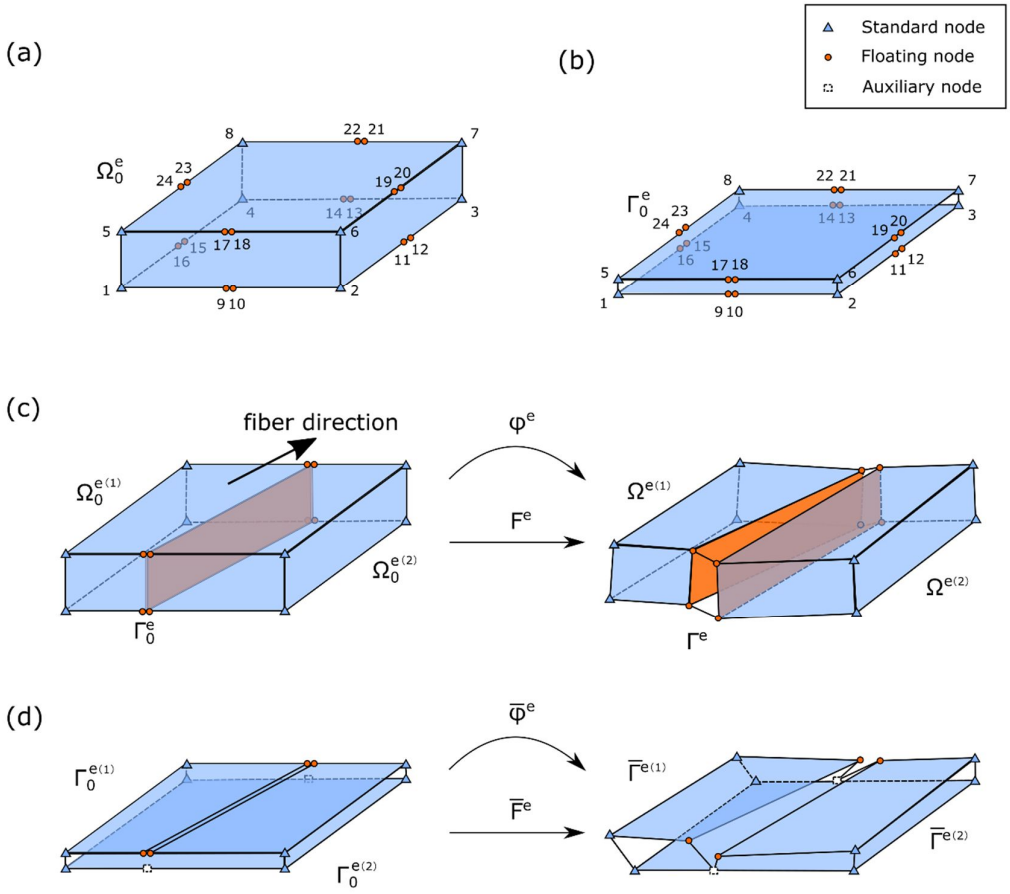

Figure 2. (a) Enriched solid element; (b) Enriched cohesive element;
(c) Configurations of a cracked solid element;
(d) Configurations of a cohesive element (considering interaction with matrix cracking).

The cracked solid element as plotted in Fig. 2 (c) consists of two standard 8-node brick elements and one 8-node cohesive elements. The deformation map of this enriched element can be given as:

$$\boldsymbol{\varphi}^e = \begin{cases} \boldsymbol{\varphi}^{e(1)}(\boldsymbol{X}): & \Omega_0^{e(1)} \to \Omega^{e(1)} \\ \boldsymbol{\varphi}^{e(2)}(\boldsymbol{X}): & \Omega_0^{e(2)} \to \Omega^{e(2)}, \end{cases} \tag{1}$$

based on which the crack surface Γ_0^e in the reference configuration may be mapped to different parts Γ_0^{e-} and Γ_0^{e+}. To define cohesive behavior, a fictitious surface is $\bar{\Gamma}^e$ is introduced and an average map is defined as:

$$\bar{\boldsymbol{\varphi}}^e = \frac{1}{2}\left(\boldsymbol{\varphi}^{e(1)}\left(\boldsymbol{X}|_{\Gamma_0^{e-}}\right) + \boldsymbol{\varphi}^{e(2)}\left(\boldsymbol{X}|_{\Gamma_0^{e+}}\right)\right) : \ \Gamma_0^e \to \bar{\Gamma}^e. \tag{2}$$

Similarly, the interface element below is also partioned in the same manner for the sake of displacement compatibility. The average map is given as:

$$\bar{\boldsymbol{\varphi}}^e = \begin{cases} \bar{\boldsymbol{\varphi}}^{e(1)}(\boldsymbol{X}): & \Gamma_0^{e(1)} \to \bar{\Gamma}^{e(1)} \\ \bar{\boldsymbol{\varphi}}^{e(2)}(\boldsymbol{X}): & \Gamma_0^{e(2)} \to \bar{\Gamma}^{e(2)} \end{cases}. \tag{3}$$

Other kinematics such as deformation gradient $\boldsymbol{F}$ and displacement jump $[\![\boldsymbol{u}]\!]$ can be defined independently in these disjoint domains.

The matrix failure onset is evaluated by a quadratic interactive criterion:

$$\left(\frac{S_{22}}{Y_T}\right)^2 + \left(\frac{S_{12}}{S_L}\right)^2 + \left(\frac{S_{13}}{S_L}\right)^2 = 1, \tag{4}$$

where $\boldsymbol{S}_{\blacksquare\blacksquare}$ is the second *Piola-Kirchhoff* stress with respect to the principal material coordinates and Y_T, S_L are transverse tensile strength and shear strength, respectively. It is assumed that cracks propagate along fiber direction and they are perpendicular to the lamina plane. The nonlinear material model for matrix cracks and interface cracks is described with a mixed-mode bilinear cohesive law [7]. The effect of through-thickness compression on the delamination initiation may be taken into account with an empirical criterion [4].

The finite element equations are formulated with the total Lagrangian formulation. The discrete residuals of enriched solid element and enriched cohesive element are expressed as the assembly of subelements:

$$\boldsymbol{R}_{\boldsymbol{ers}}^{\boldsymbol{e}} = \mathcal{A}\left(\boldsymbol{R}_{\boldsymbol{s}}^{\boldsymbol{e}}|_{\Omega_0^{e(1)}},\ \boldsymbol{R}_{\boldsymbol{s}}^{\boldsymbol{e}}|_{\Omega_0^{e(2)}},\ \boldsymbol{R}_{\boldsymbol{c}}^{\boldsymbol{e}}|_{\Gamma_0^{e}}\right), \tag{5}$$

$$\boldsymbol{R}_{\boldsymbol{erc}}^{\boldsymbol{e}} = \mathcal{A}\left(\boldsymbol{R}_{\boldsymbol{c}}^{\boldsymbol{e}}|_{\Gamma_0^{e(1)}},\ \boldsymbol{R}_{\boldsymbol{c}}^{\boldsymbol{e}}|_{\Gamma_0^{e(2)}}\right), \tag{6}$$

where $\boldsymbol{R}_{\boldsymbol{s}}^{\boldsymbol{e}}$ and $\boldsymbol{R}_{\boldsymbol{c}}^{\boldsymbol{e}}$ denote residuals of standard solid element and standard cohesive element. Finally, the FE equations of the dynamic problem can be written as:

$$\boldsymbol{M}\ddot{\boldsymbol{d}} + \boldsymbol{F}_{\text{int}}(\boldsymbol{d}) + \boldsymbol{F}_{\text{coh}}(\boldsymbol{d}) - \boldsymbol{F}_{\text{ext}} = 0, \tag{7}$$

where $\boldsymbol{d}$ is nodal displacement, $\boldsymbol{M}$ is mass matrix, $\boldsymbol{F}_{\text{int}}$, $\boldsymbol{F}_{\text{coh}}$ and $\boldsymbol{F}_{\text{ext}}$ denote internal force of solid elements, interface elements and external force, respectively. An implicit time integration with *Hilber-Hughers-Taylor* operator was adopted in the current work for the solution of Eq. (7).

3.2. Finite element model

The experiment of LVI on a $[0_3/90_3]_s$ laminate [4] is adopted for the verification of the method proposed here. As shown in Fig. 3 (a), a rectangular laminate plate (65 mm×87.5 mm×2 mm) placed on a steel plate with a 45 mm×67.5 mm rectangular opening was impacted by a 2.3kg falling mass with a hemispherical nose steel tup of 12.5mm diameter. Impact energies varying from 0.5J to 7J have been tested in [4] and a typical result with 6J impact energy is chosen in this study. The FE model of the laminate is illustrated in Fig. 3 (b). Three enriched solid elements are used through thickness for three blocks of plies (0_3, 90_6, 0_3) and two enriched cohesive elements model two interfaces. For the sake of efficiency, only the center region is discretized with a fine mesh (0.5 mm×0.5 mm) and the boundary condition is simplified by constraining the nodes of the laminate corresponding to the edge of support plate (u_x=u_y=u_z=0). The impactor is discretized with ABAQUS R3D4 rigid elements and contact pairs are defined between the top surface of the laminate and the outer surface of the impactor. The material properties for solid elements and cohesive elements are listed in Table 1. In the current study, the top 0^o plies are assumed to be intact with no cracks. The total simulation time for the dynamic analysis is 6 ms.

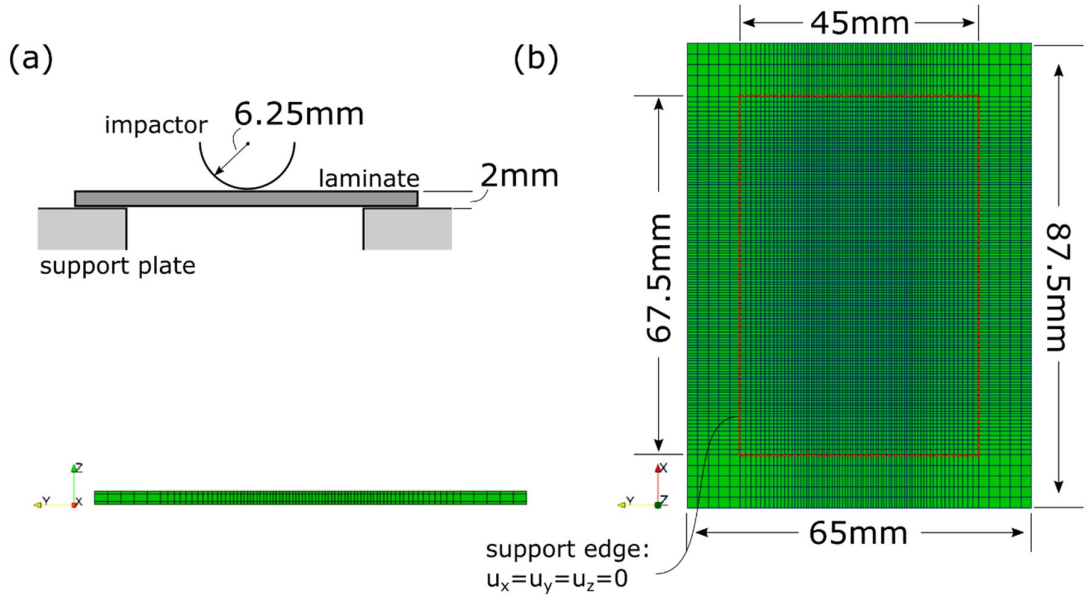

Figure 3. (a) Experimental setup [4]; (b) FE model of the laminate.

Table 1. Material properties used in the simulations.

Solid element		Cohesive element	
E_{11} (GPa)	93.7	$k_N=k_S=k_T$ (N/mm^3)	10^6
$E_{22}=E_{22}$ (GPa)	7.45	Y_T (MPa)	30
$G_{12}=G_{23}=G_{13}$ (GPa)	3.97	S_L (MPa)	80
$v_{12}=v_{23}=v_{13}$	0.261	G_{IC} (KJ/m^2)	0.520
-	-	$G_{IIC}= G_{IIIC}$ (KJ/m^2)	0.970

4. Results and discussion

The simulation results are compared against experimental results in terms of force vs. time curves and damage patterns as shown in Fig. 4 and Fig. 5, respectively. The predicted structural response curve agrees well with the experimental curve but the peak force is over predicted since fiber damage and the damage on the top layer are ignored in the current simulation. The through-thickness impact damage maps including delamination and matrix cracks are plotted in Fig. 5 (b)-(e). A symmetry delamination with the major axis oriented along 0^o direction is observed on the lower interface with comparable shape and size against the experimental result. Subtle features like pointed delamination tip and partial intact zone in the central region as mentioned in [7] are well captured. On the upper interface, the delamination is totally suppressed right below the impactor due to the compressive stress. The shape of slight delaminations at two sides indicates they propagate along 90^o direction. The matrix cracks are shown in Fig. 5 (d) and (e), where a major bending crack is found in the bottom layer with several shear cracks observed in the middle layer. Simulations indicate bending cracks are firstly initiated and shear cracks emerge afterwards, which trigger the delamination on the interfaces right above corresponding layers.

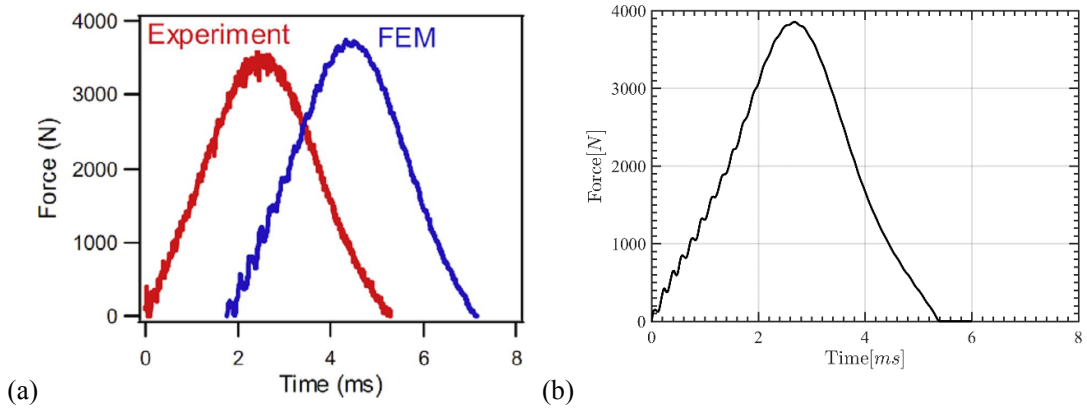

Figure 4. Force versus time curves (a) experiment [4], (b) simulation.

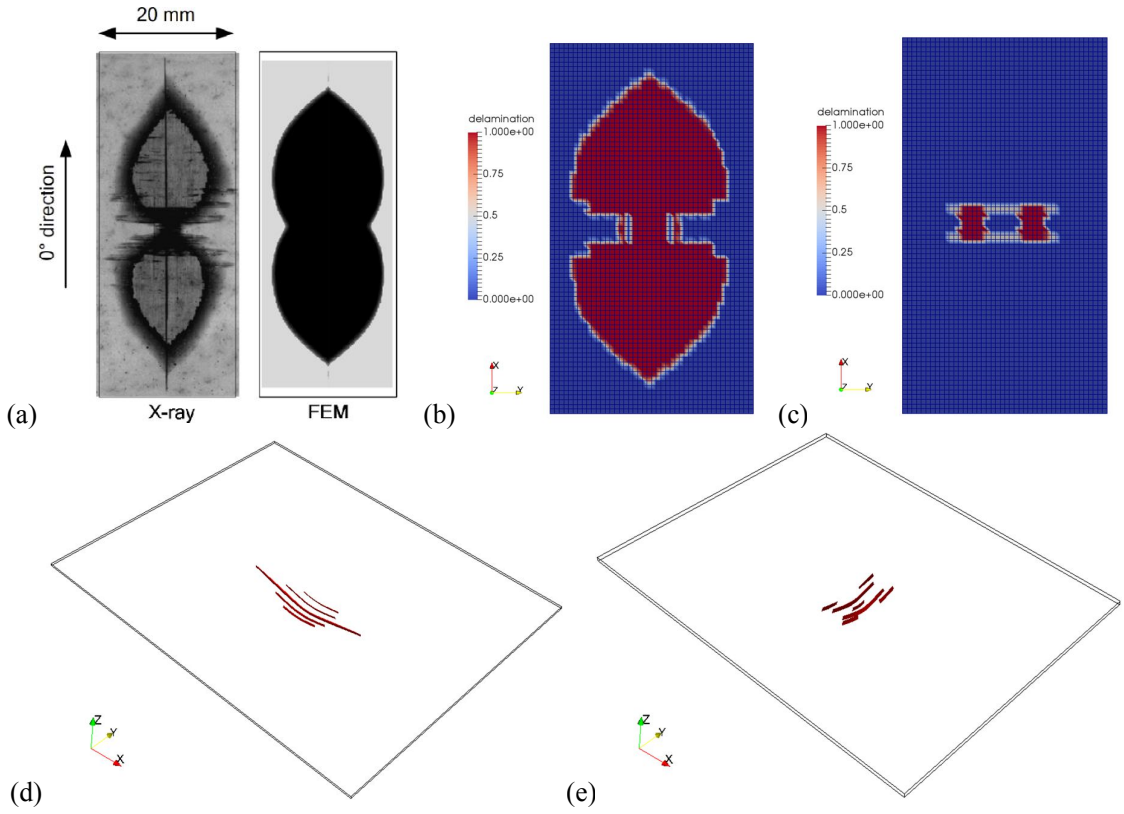

Figure 5. Delamination on the lower 90/0 interface (a) experiment [4], (b) simulation;
(c) Delamination on the upper 0/90 interface;
(d) Bending cracks on the bottom layer;
(e) Shear cracks on the middle layer.

5. Conclusions

A discrete crack model of damage in composite laminates subjected to low velocity impact is presented by applying the recently-developed *Floating Node Method* extended for geometrically nonlinear dynamic analysis. In the current study, matrix cracking and delamination are assumed as the only damage mechanisms evolved in the impacted laminate, for which enriched solid elements and

enriched cohesive elements are formulated based on the FNM concept. Interaction between matrix cracking and delamination is automatically considered in the formulated enriched elements. Based on this proposed method, the LVI impact damage of a typical cross-ply laminate has been modelled, which shows accurate results in terms of the force response curves and damage patterns. Two lobes of delamination in the typical peanut shape, bending cracks and shear cracks are successfully captured. In future work, the analysis will be extended to laminates with general ply sequences and higher impact energies.

References

[1] Abisset E, Daghia F, Sun XC, Wisnom MR, Hallett SR. Interaction of inter- and intralaminar damage in scaled quasi-static indentation tests: Part 1 - Experiments. *Compos Struct*. 2016; 136: 712-26.

[2] Abir MR, Tay TE, Ridha M, Lee HP. Modelling damage growth in composites subjected to impact and compression after impact. *Compos Struct*. 2017; 168: 13-25.

[3] Abir MR, Tay TE, Ridha M, Lee HP. On the relationship between failure mechanism and compression after impact (CAI) strength in composites. *Compos Struct*. 2017; 182: 242-50.

[4] Aymerich F, Dore F, Priolo P. Simulation of multiple delaminations in impacted cross-ply laminates using a finite element model based on cohesive interface elements. *Compos Sci Technol*. 2009; 69: 1699-1709.

[5] Sun XC, Wisnom MR, Hallett SR. Interaction of inter- and intralaminar damage in scaled quasi-static indentation tests: Part 2-Numerical simulation. *Compos Struct*. 2016; 136: 727-42.

[6] Sitnikova E, Li S, Li D, Yi X. Subtle features of delamination in cross-ply laminates due to low speed impact. *Compos Sci Technol*. 2017; 149: 149-58.

[7] Chen BY, Tay TE, Pinho ST, Tan VBC. Modelling the tensile failure of composites with the floating node method. *Comput Method Appl M*. 2016; 308: 414-42.